The Journal of Experimental Biology 206, 1449-1460

doi:10.1242/jeb.00234

Localization of myoinhibitory peptide immunoreactivity in *Manduca sexta* and *Bombyx mori*, with indications that the peptide has a role in molting and ecdysis

Norman T. Davis[1,*], Michael B. Blackburn[2], Elena G. Golubeva[2] and John G. Hildebrand[1]

[1]*Division of Neurobiology, University of Arizona, Box 210077, Tucson, AZ 85721-0077, USA* and [2]*Insect Biocontrol Laboratory, USDA, ARS, PSI, BARC-West, Beltsville, MD 20705, USA*

*Author for correspondence (e-mail: ntd@neurobio.arizona.edu)

Accepted 13 January 2003

Summary

For normal development of *Manduca sexta* larvae, the ecdysteroid titer must drop following its sudden rise at the start of the molting cycle; this sudden decline in titer may be due to myoinhibitory peptide I (MIP I), which has an inhibitory effect on the release of ecdysone by the prothoracic glands of *Bombyx mori in vitro*. Using an antiserum to MIP, we have demonstrated secretion of an MIP-like peptide by the epiproctodeal glands of *Manduca sexta*, which are located on each proctodeal nerve, just anterior to the rectum. These MIP-immunoreactive glands are also present in *B. mori*. In fourth-instar larvae of *M. sexta*, the epiproctodeal glands show a distinct cycle of synthesis and sudden release of MIP that coincides with the time of the rapid decline in ecdysteroid titer. The function of the epiproctodeal glands appears to be the timely release of MIP during the molting cycle, so as to inhibit the prothoracic glands and thus to facilitate the sudden decline in ecdysteroid titer. In addition, we have found that MIP immunoreactivity is co-localized with that of crustacean cardioactive peptide (CCAP) in the 704 interneurons; these peptides appear to be co-released at the time of ecdysis. It is known that CCAP can initiate the ecdysis motor program; our results suggest that MIP may also be involved in activating ecdysis behavior.

Key words: tobacco hornworm, *Manduca sexta*, *Bombyx mori*, CCAP, ecdysteroids, prothoracicostatic peptide, ecdysterostatic hormone, neurosecretion, allatostatin, epiproctodeal gland.

Introduction

Hormonal regulation of molting and metamorphosis in *Manduca sexta* has been studied extensively and shown to be primarily under the control of juvenile hormone (JH) and ecdysteroids (reviewed by Nijhout, 1994; Gäde et al., 1997). During larva–larva molts, the release of ecdysteroids signals the end of the feeding stage and the initiation of the molting process, and, in the presence of JH, growth is directed to the expression of larval characteristics. Near the end of the feeding stage of the final (fifth) larval instar, a small ecdysteroid peak in the absence of JH commits the larva to development of pupal characteristics; in the pre-pupal stage that follows, an ecdysteroid peak accompanied by an increase in JH titer initiates pupal development. In the pupal stage, a prolonged ecdysteroid peak in the absence of JH initiates adult development.

In the later stages of adult development there is a rapid decline in ecdysteroid titer, and this decline has been shown to be essential for initiating the programmed cell death that accompanies adult metamorphosis (Schwartz and Truman, 1983). During the molt from the fourth to the fifth larval instar, the drop in the ecdysteroid peak is even more precipitous (Bollenbacher et al., 1981; Langelan et al., 2000). This rapid decline in ecdysteroid titer is essential for activating endocrine cells that initiate ecdysis behavior (Sláma, 1980; Truman et al., 1983; Truman and Morton, 1990; Hewes and Truman, 1994; Žitňan et al., 1999; Kingan and Adams, 2000). In addition, the decline in ecdysteroid titer is essential for the initiation of cuticular melanization in larvae (Curtis et al., 1984).

The rapidly rising phase of the ecdysteroid titer results from activation of the prothoracic glands by prothoracicotropic hormone (PTTH; see review by Bollenbacher and Granger, 1985). Several factors that inhibit rather than stimulate ecdysteroid production have been identified in insects (reviewed by Gäde et al., 1997; Hua et al., 1999; Dedos et al., 2001), and these factors may be involved in promoting the rapidly declining phase of the ecdysteroid peaks. A neuropeptide that acts, *in vitro*, on the prothoracic glands to inhibit PTTH-stimulated secretion of ecdysone by the silkworm *Bombyx mori* is of special interest to our study (Hua et al., 1999; Dedos et al., 2001). Hua et al. (1999) found this prothoracicostatic peptide to be identical to a myoinhibitory peptide, Mas-MIP I (*Manduca sexta* myoinhibitory peptide I), which was first isolated and identified from *M. sexta* by Blackburn et al. (1995).

Mas-MIP I belongs to the W2W9amide peptide family that is characterized by tryptophan residues at the 2 and 9 positions (Lorenz et al., 2000). Peptides of this family have been identified in a locust (Schoofs et al., 1991), moths (Blackburn

et al., 1995, 2001; Hua et al., 1999), a cricket (Lorenz et al., 1995), a stick insect (Lorenz et al., 2000) and a cockroach (Predel et al., 2001). In addition, a gene for these peptides was cloned in *B. mori* (Hua et al., 2000) and *Drosophila melanogaster* (Williamson et al., 2001). These various reports suggest that the W2W9amide peptides are of widespread occurrence in insects. Moreover, bioassays indicate that, in addition to the prothoracicostatic effect mentioned above, these peptides may inhibit myogenic contraction of visceral muscles in locusts, moths and cockroaches (Schoofs et al., 1991; Blackburn et al., 1995; Predel et al., 2001) and JH and ovarian ecdysteroid synthesis in crickets (Lorenz et al., 1995, 2000).

As yet, the endocrinal source of the MIP/prothoracicostatic peptide has not been demonstrated conclusively. Triseleva and Golubeva (1998), using an antiserum raised to Mas-MIP I, found MIP-immunoreactive (MIP-IR) cells in the subesophageal and abdominal ganglia and on the hindgut of adults of the tobacco budworm *Heliothis virescens,* and Hua et al. (2000) labeled a pair of MIP-IR neurosecretory cells in the brain of *B. mori*. Therefore, using an antiserum to Mas-MIP I (Triseleva and Golubeva, 1998), we have undertaken to identify the MIP-IR neuroendocrine cells that may be a source of an MIP/prothoracicostatic hormone in *M. sexta.* The principal focus of our study has been the fourth-instar larval stage, because the hormonal control of molting of this stage has been well studied and because this stage is uncomplicated by metamorphic changes. We have also examined MIP immunoreactivity in fourth-instar larvae of *B. mori*.

Materials and methods

Animals

Manduca sexta L. used in our experiments were obtained from a laboratory colony maintained as described previously (Davis et al., 1997). In both the colony and in experiments, larvae were reared on an artificial diet, and larvae and adults were kept at 25°C, 50–60% relative humidity and on a short-day photoperiod (12 h:12 h L:D). The start of the scotophase was arbitrarily designated as hour 00.00 of each new day. The day of ecdysis to the next instar was designated as day 0.

Eggs of *Bombyx mori* L. were obtained from Carolina Biological Supply Company (Burlington, NC, USA), and the larvae were fed freshly collected mulberry leaves and kept under the same conditions as above.

Staging of fourth-instar larvae of M. sexta

Fourth-instar larvae were used to study the secretory cycle of the MIP-immunoreactive (MIP-IR) epiproctodeal gland. This instar may be divided into pre-molting and molting phases, and the initiation of the molting phase is photo-gated. Molting of Gate I, fourth-instar larvae begins with the release of PTTH late in the second scotophase after ecdysis, and molting of Gate II larvae begins with release of PTTH early in the third scotophase (Truman, 1972). Gate II larvae were used to study the epiproctodeal glands during the molting cycle because the onset of the cycle is well synchronized by the photo-gate. Groups of Gate II larvae were isolated by the method described by Fain and Riddiford (1975). Glands from day 0, day 1 and day 2 of Gate II larvae were used to study the pre-molting phase of the instar.

In order to study the glands at specific stages during the molting phase, we used the external markers described by Fain and Riddiford (1975), Curtis et al. (1984) and Langelan et al. (2000). These markers are based on: (1) separation of the seventh abdominal spiracular plate from the old cuticle (spiracular apolysis) and subsequent development of this pharate spiracular plate of the fifth-instar larva; (2) slippage of the pharate head capsule; (3) tanning of the pharate crochets of the prolegs; and (4) appearance of air in the old head capsule (airheads) shortly before ecdysis to the fifth instar.

Endocrine glands from the following stages of molting were studied: (1) early onset of spiracular apolysis, which begins several hours after the release of PTTH and is recognized by a gradual lightening of color in a small, crescent-shaped area immediately above the spiracle (Langelan et al., 2000); (2) approximately 4 h prior to head-capsule slippage, the time at which the pharate spiracular plate is approximately 250 μm longer than that of the fourth-instar larva; (3) onset of head-capsule slippage, which occurs approximately 12 h after the onset of spiracular apolysis and is recognized by the separation of the stemmata from the old cuticle, as the pharate head begins a slow retraction into the prothoracic exoskeleton of the fourth-instar larva; (4) 5 h and (5) 10 h after the onset of head-capsule slippage, stages which were obtained by timing larvae from the onset of head-capsule slippage; (6) tanning of the crochets, which occurs approximately 18 h after head-capsule slippage; and (7) airheads, which appear approximately 28 h after the onset of head-capsule slippage.

Immunocytochemistry

The insects were anesthetized by chilling on crushed ice, and tissues were dissected in cold, physiological saline solution (Pichon et al., 1972). The tissues were then fixed for 12 h in cold 4% paraformaldehyde and immunostained as whole mounts or as 200-μm sections cut on a Vibratome (Technical Products International, St Louis, MO, USA). The fluorescence immunocytochemistry was performed as described previously (Davis et al., 1993). Briefly, the tissues were processed as follows. After fixation and after incubations in the primary and secondary antisera, respectively, the tissues were washed thoroughly in phosphate-buffered saline (pH 7.2) containing 1% Triton X-100 (PBST). Normal donkey serum (10%) in PBST was used as the blocking solution and as the diluent for the various antisera. The polyclonal antiserum to Mas-MIP I was raised as described by Triseleva and Golubeva (1998) and, using whole mounts of the CNS of third-instar larvae of *M. sexta*, we tested the immunostaining by this antiserum at dilutions ranging from 1:500 to 1:10 000. Because a dilution of 1:2000 appeared to give optimum results, this dilution of the antiserum was used routinely. It was applied for approximately 12 h at room temperature and with gentle rotation. In addition, antisera to a cockroach-type allatostatin, to crustacean

cardioactive peptide (CCAP) and to molluscan small cardioactive peptide B (SCP_B) were used under the same conditions. Goat anti-rabbit immunoglobulin G (IgG) conjugated to tetramethyl rhodamine isothiocyanate (TRITC) or to fluorescein isothiocyanate (FITC), and goat anti-mouse IgG conjugated to FITC (Jackson ImmunoResearch Laboratories, West Grove, PA, USA) were used as secondary antisera and applied at a dilution of 1:200 for 12 h at room temperature and with gentle rotation.

Double-immunostaining to identify the MIP-IR neuroendocrine cells of the adult brain was accomplished using the rabbit polyclonal antiserum to MIP and the mouse monoclonal antibody to SCP_B, and these antisera were labeled, respectively, with TRITC-conjugated goat anti-rabbit IgG and FITC-conjugated goat anti-mouse IgG. In addition, double-staining of neuroendocrine cells was performed using FITC-conjugated, goat anti-rabbit IgG to label the anti-MIP, and then, after treatment with normal rabbit serum to block any unbound goat anti-rabbit IgG binding sites, the tissue was immunostained with TRITC-conjugated, rabbit anti-allatostatin (Davis et al., 1997). The method described by Nichols et al. (1995a,b) was used for double-immunostaining for CCAP (Davis et al., 1993) and MIP. The tissue was first treated with a rabbit antiserum to CCAP and labeled with an excess (1:100) of Rhodamine Red-X-conjugated Fab fragment of anti-rabbit IgG (H+L) from goat (Jackson ImmunoResearch Laboratories). Then, after thorough washing, the tissue was treated with rabbit antiserum to MIP and labeled with FITC-conjugated anti-rabbit IgG from goat.

To test the capacity of the MIP antiserum to recognize epitopes of Mas-MIP I, the working dilution of the antiserum was subjected to liquid-phase preadsorption for 24 h at 4°C in 10^{-4} mol l^{-1} synthetic Mas-MIP I; this treatment eliminated all specific immunostaining. Davis et al. (1993, 1997) previously characterized the immunostaining of *M. sexta* tissues by antisera to CCAP and allatostatin and to the antibody to SCP_B.

In addition to the immunostaining, the RNA in the gland cells was stained with Acridine Orange according to the histochemical method of Kiernan (1990).

Neuronal tracing

The axonal projections to their targets (orthograde) were traced by filling through stumps of the proctodeal nerve. Biocytin (Sigma, St Louis, MO, USA) was used for filling towards peripheral targets and was labeled with TRITC-conjugated streptavidin (Jackson ImmunoResearch Laboratories), following the methods of Consoulas et al. (1999). The filling period was 1–2 days at approximately 5°C.

Laser scanning confocal microscopy

Digitized images of the immunostained and filled preparations were obtained using a Nikon E800 confocal microscope equipped with green He/Ne and argon lasers and the appropriate filters. Optical sections (5 μm**)** of digitized images were merged and processed using software programs of Simple PCI (Compix Inc., Cranberry Township, PA, USA), Corel Draw and Corel Photopaint (Corel Corp., Ottawa, Ontario, Canada). Prints were made using a Tektronix Phaser SDX. Where needed, the digitized images were modified only to merge files, enhance contrast and provide color.

Results

MIP-IR neurons in the CNS of larval M. sexta

MIP-immunostaining of whole mounts of the CNS of third- and fourth-instar larvae labeled an assortment of small neurons in the brain (Fig. 1A). These cells appeared to be interneurons in that they were small and did not project to peripheral targets. No MIP-IR neurohemal processes were found in the corpus cardiacum or corpus allatum (Fig. 1B). Therefore, the brain–retrocerebral complex did not appear to be involved in the production and release of an MIP-like neurohormone.

Because no MIP-immunoreactive neurons were found in the frontal ganglion or in the recurrent nerve (not shown), it appears that MIP does not function as a myoactive peptide in the stomatogastric nervous system.

Ganglia of the larval ventral nerve cord contained several MIP-IR somata, and, of these, a pair of MIP-IR neurons in the abdominal ganglia were identified as the 704 interneurons (Fig. 1C). These cells are discussed in further detail below. Neurons of the ventral nerve cord cells did not project to the perivisceral organs (PVO; Fig. 1C), and, thus, there was no evidence of release of MIP-IR neuropeptides from neuroendocrine cells into the ventral nerve cord of larvae. Except for the terminal abdominal ganglion (TAG), MIP-IR processes did not extend into nerves of the ganglia of the ventral nerve cord. Therefore, there was no evidence that MIP-IR neurons in these pre-terminal ganglia innervate any peripheral organs, including the prothoracic glands.

The MIP antiserum labeled several large, mid-line and lateral neurons in the TAG (Fig. 1D), and processes of these cells extended into dorsal nerve 8 (curved arrow) and the terminal nerve (straight arrow). These MIP-IR cells will be considered in a separate publication, but it should be noted here that they do not project to neurohemal release sites and, thus, are not neuroendocrine. Instead, they mostly innervate muscles of the hindgut (Fig. 1E) *via* projections into the terminal nerve and thence into the proctodeal nerve. The larval hindgut and its innervation by the proctodeal nerve are depicted in Fig. 2.

The epiproctodeal glands of M. sexta *larvae*

The antiserum to MIP labeled two pairs of large, multinuclear, neuroendocrine cells on the proctodeal nerve of all larval and pupal stages. Although these are peripheral neurosecretory cells, we will show that they have a very specialized structure and a secretory function that appears to be independent of the nervous system. We therefore have chosen to name them the epiproctodeal glands. Each gland is attached to the proctodeal nerve just anterior to the junction of the rectum and hindgut (Figs 2, 3A) and, at this location, the gland and proctodeal nerve are anchored tightly to the hindgut by connective-tissue fibers. The structure of the cells of this

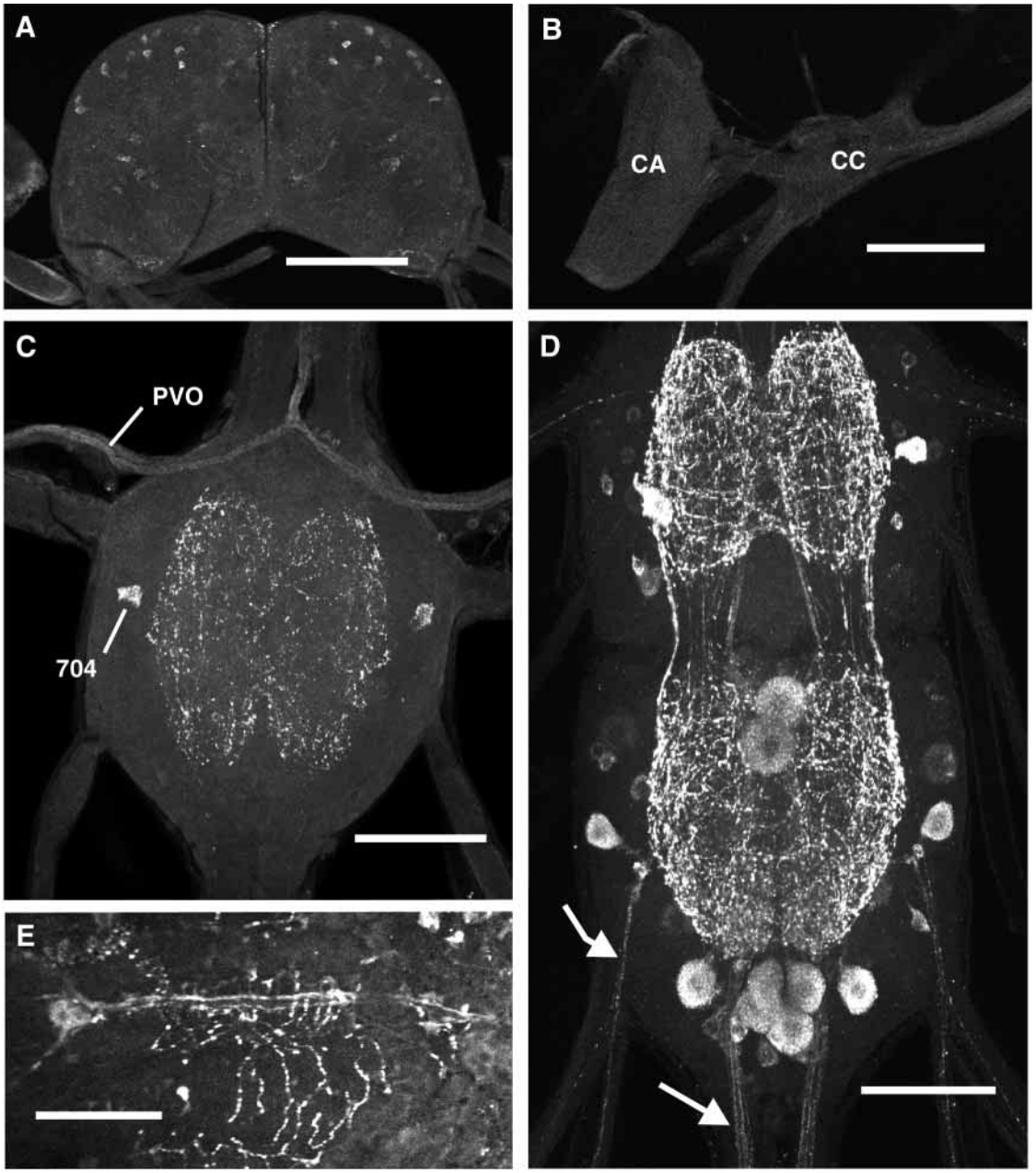

Fig. 1. Confocal images of myoinhibitory peptide (MIP)-immunostained whole mounts of larval organs of *Manduca sexta*. (A) Brain of a third-instar larva, showing numerous small, MIP-immunoreactive neurons; the size and location of these cells indicate that they are not neurosecretory cells. (B) Corpus allatum (CA) and corpus cardiacum (CC) of an early fifth-instar larva, showing a lack of immunoreactive neurohemal processes. (C) Third abdominal ganglion of a third-instar larva, showing a pair of interneurons (704) and a lack of immunoreactive neurohemal processes in the perivisceral organ (PVO). (D) Terminal abdominal ganglion of a third-instar larva showing lateral cells that project into the eighth dorsal nerve (curved arrow) and a terminal cluster of mid-line neurons that project into the terminal nerve (straight arrow). (E) MIP-immunoreactive endings on muscles of the posterior region of the hindgut. Scale bars, 100 μm.

neuroendocrine gland were first described by Reinecke et al. (1978), who noted that they are multinucleate (Fig. 3B) and contain many dense-core vesicles.

Many varicose processes extend from the gland cells onto the surface of the proctodeal nerve and its branches (Fig. 3A). These processes do not extend onto the terminal nerve, and no processes were found extending onto the musculature of the hindgut. These superficial, varicose processes are typical of those known to serve for neurohemal release; therefore, the immunoreactivity of the epiproctodeal glands indicates that they release an MIP-like peptide into the hemolymph.

Because backfills from the base of the terminal nerve to the proctodeal nerve did not stain the cells of the epiproctodeal gland, we concluded that processes of these cells do not extend

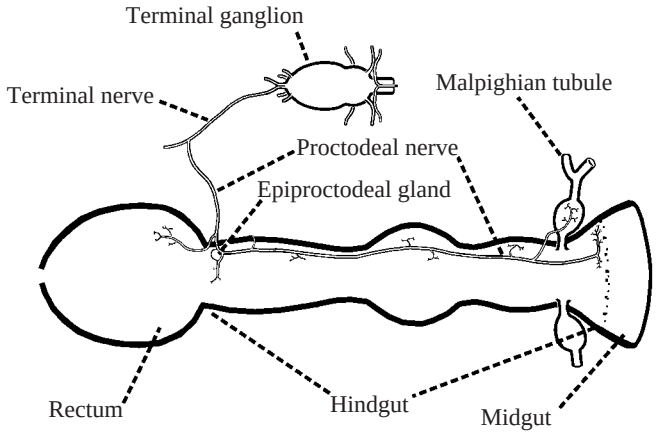

Fig. 2. A depiction of larval hindgut innervation by the proctodeal nerve and the location of the epiproctodeal gland.

into the TAG (Fig. 3C). Moreover, these preparations showed that axons from the TAG do not innervate the epiproctodeal glands (Fig. 3C).

While immunostaining the epiproctodeal glands, we noted that their appearance changed during the course of the fourth larval instar. We therefore wished to determine if this variation might represent stages of synthesis and release of neurosecretory products. In order to obtain comparable staining of glands at various stages of the instar, we used identical processing and MIP-immunostaining schedules as well as identical gain and black-level settings for the confocal images. Ten or more glands were stained at each of the three pre-molting and seven molting stages indicated in the Materials and methods. Each image shown in Fig. 4 and Fig. 5 was selected as representative of the designated stage in the pre-molting or molting phases of the fourth-instar larva.

On day 0, the immunostaining of the neurohemal system of the epiproctodeal gland was distinct (Fig. 4A) and, by the onset of spiracular apolysis, the staining had become intense (Fig. 4B). At approximately 4 h before head-capsule slippage, the immunostaining of the neurohemal system appeared to show a moderate decline (Fig. 4C), and at this time many of the varicosities appeared to be partly vacuous (Fig. 4I). By the onset of head-capsule slippage, the decline in immunostaining was pronounced (Fig. 4D). Five hours after head-capsule slippage, most of the immunostaining of the neurohemal system had disappeared (Fig. 4E), but the cell bodies had become intensely immunoreactive (arrow). The extent of immunostaining of the neurohemal system appeared to increase somewhat by 10 h after head-capsule slippage (Fig. 4F) and had increased conspicuously by the stage of tanning of the crochets (Fig. 4G). By the airhead stage, the immunostaining of the gland (Fig. 4H) was comparable to that of the gland in the pre-molting phase fourth-instar larvae (Fig. 4A).

The intensity of immunostaining of the epiproctodeal-gland cells also appeared to undergo changes related to the pre-molting and molting stages of the fourth larval instar. Images of these changes were recorded using a 5-μm, optical section made near the middle of typical gland cells of each stage and using the same settings of the confocal microscope for each image. The intensity of MIP-immunostaining of the cytoplasm was low during the pre-molting stage (Fig. 5A,B), but staining became distinctly stronger by the onset of spiracular apolysis (Fig. 5C). By the onset of head-capsule slippage (Fig. 5D), and continuing for at least 5 h (Fig. 5E), the immunostaining of the cytoplasm was intense. Ten hours after head-capsule slippage, the staining had decreased (Fig. 5F), and this decrease in staining continued at the crochet-tanning (Fig. 5G) and airhead (Fig. 5H) stages to become comparable to the staining of the cells at the pre-molting stage.

MIP-IR neuroendocrine cells of adult M. sexta

Immunostaining of Vibratome sections of the brain of adults demonstrated two pairs of MIP-IR median neurosecretory cells in the brain (Fig. 3D; green), and the processes of these cells were found to project to neurohemal release sites in the corpora cardiaca (Fig. 6A). In *M. sexta*, there are only two groups of median neuroendocrine cells present as two pairs, the type $1A_4$ and $1A_5$ cells (Homberg et al., 1991). The $1A_5$ cells are labeled uniquely by the monoclonal antibody to SCP_B (Davis et al., 1997) and can be distinguished, thereby, from the $1A_4$ cells. Vibratome sections were double-labeled using rabbit anti-MIP and mouse anti-SCP_B, as indicated in the Materials and methods. The results shown in Fig. 3D indicated that the MIP-IR staining (green) is not co-localized with the SCP_B-IR staining (red) of the $1A_5$ cells (Fig. 3D), and the MIP-IR neuroendocrine cells must, therefore, be the $1A_4$ cells. The $1A_4$ cells are also known to be allatostatin-immunoreactive (Davis et al., 1997) and, as further proof of the identity of the MIP-IR neuroendocrine cells, brain sections were doubly stained for allatostatin and MIP. The results indicated that allatostatin and MIP immunoreactivities are co-localized in the $1A_4$ neurosecretory cells (Fig. 3E, yellow).

In adults, as in larvae, no evidence was found of neurohemal release of MIP from the abdominal ganglia (Fig. 6B–D). About mid-way in the development of the pharate adult, two pairs of neurons, additional to the 704 interneurons of larvae, were labeled for MIP-IR, but their projections indicated that they are interneurons rather than neuroendocrine cells (Fig. 6B). By near the time of adult eclosion, the immunoreactivity of all of these cells had decreased markedly (Fig. 6C) such that, in the fully mature adult, there was almost no MIP immunoreactivity in the abdominal ganglia (Fig. 6D). In the TAG of the pharate adult near mid-way in development, the interneurons, as well as the visceromotor neurons that innervate the hindgut, were weakly labeled (Fig. 6E), and in the fully mature adult, there was almost no MIP immunoreactivity in the TAG (Fig. 6F).

The epiproctodeal glands persisted in the pupa and developing, pharate adult (Fig. 6G). In addition to the nerves of the hindgut, a very extensive meshwork of MIP-IR neurohemal processes developed on each side of the anterior rectal chamber (Fig. 6G,H), and, as in the larval stage, these processes originated from the epiproctodeal gland cells. By

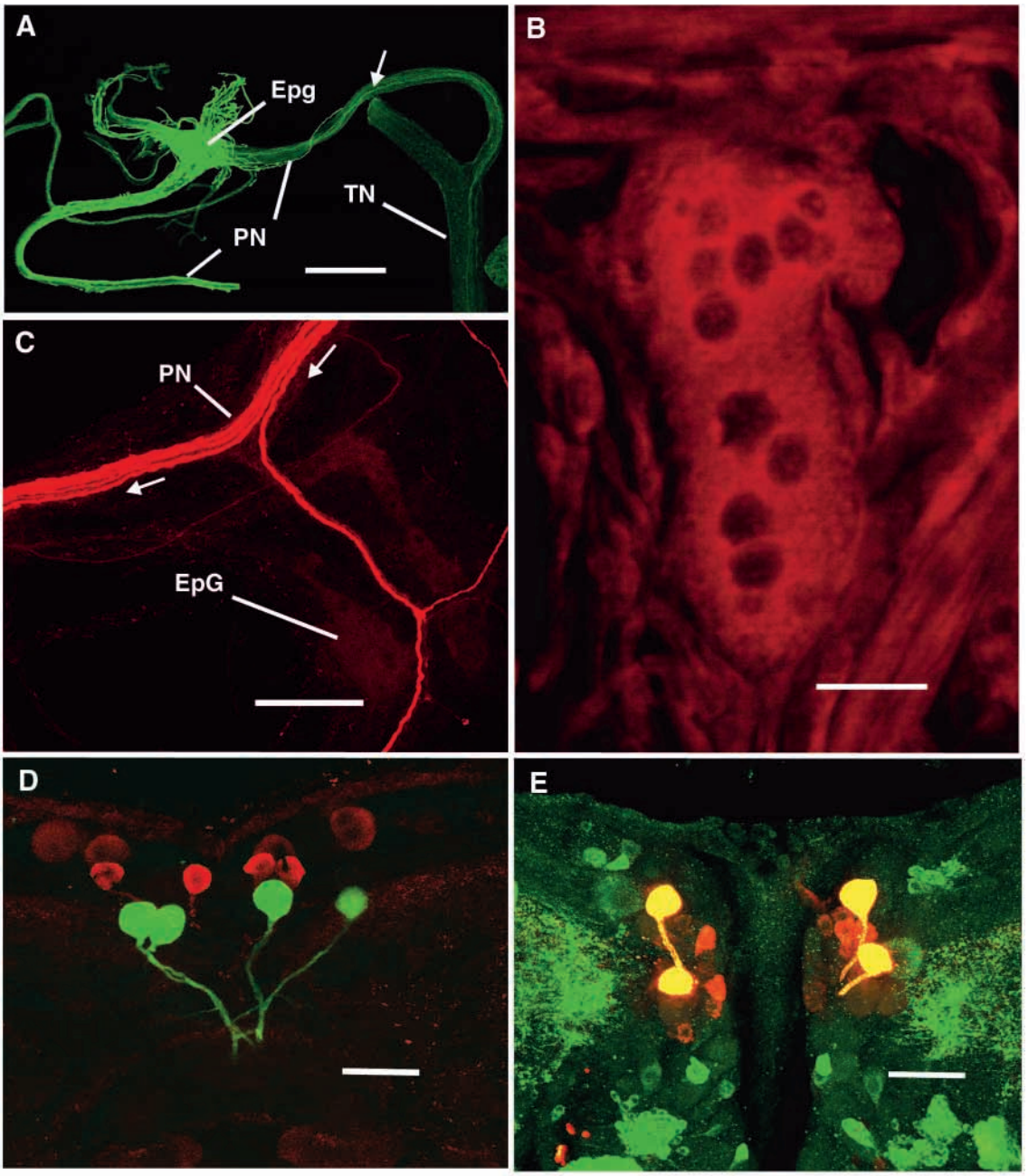

Fig. 3. Confocal images of the larval epiproctodeal gland (A,B), axons in the proctodeal nerve (C) and median neuroendocrine cells in the adult brain of *Manduca sexta* (D,E). (A) Myoinhibitory peptide (MIP)-immunostaining of a whole mount of the epiproctodeal gland (EpG) and its neurohemal processes on the proctodeal nerve (PN) of a third-instar larva. In addition, MIP-immunoreactive (MIP-IR) axons that extend from neurons in the terminal ganglion and terminal nerve (TN) can be seen in the proctodeal nerve (arrow). (B) Acridine Orange staining of a cell in a whole mount of an epiproctodeal gland of a fourth-instar larva at a late stage of spiracular apolysis. The stain demonstrates a high concentration of RNA in the cytoplasm at this stage; the unstained spherical structures in the cell have been shown in previous studies to be nuclei. (C) Whole mount of a Biocytin-stained, proctodeal nerve filled from the base of the terminal nerve of a fourth-instar larva. The location of one of the gland cells (EpG) can be distinguished by its weak background staining. Arrows indicate the direction of filling with Biocytin. Note that branches of these axons do not terminate on the epiproctodeal gland, and, therefore, the gland apparently is not innervated. Moreover, the staining failed to demonstrate any processes extending from the gland to the terminal abdominal ganglion. (D) Double-immunostaining of MIP-IR (red) in the $1A_4$ cells and of small cardioactive peptide B (SCP_B)-IR (green) in the $1A_5$ median neuroendocrine cells. Vibratome section (200 μm), frontal plane of the adult brain. (E) Double-immunostaining for MIP (red) and allatostatin (green), showing that immunoreactivity to these two peptides is co-localized (yellow) in the $1A_4$ cells. Vibratome section (200 μm), frontal plane of the adult brain. Scale bars, 400 μm (A) and 100 μm (B–E).

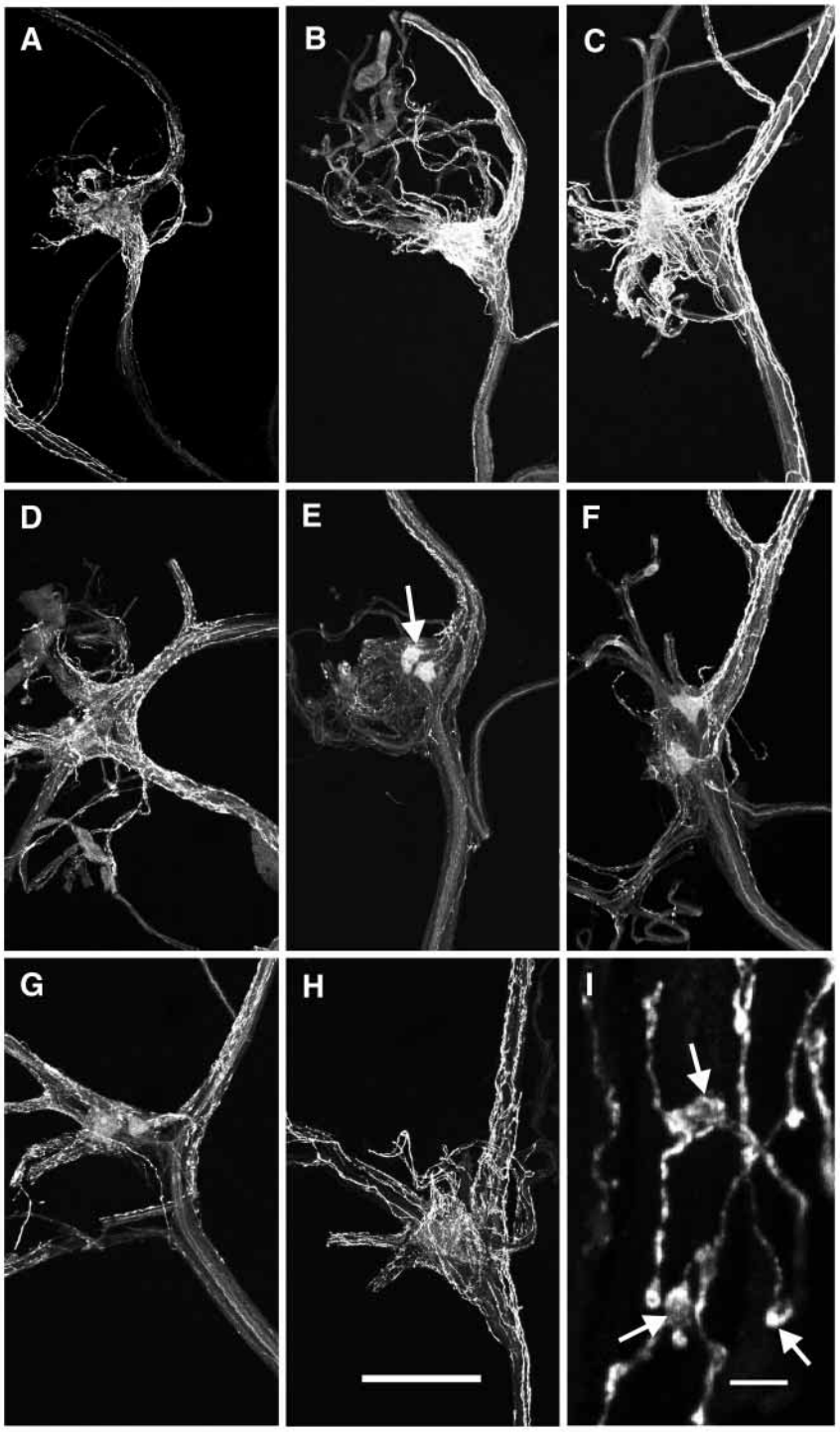

Fig. 4. Confocal images of whole mounts of epiproctodeal glands immunostained at various times in the molting cycle of fourth-instar larvae, showing a cycle of depletion and subsequent recovery of myoinhibitory peptide (MIP)-like immunoreactivity in the neurohemal system. (A) Moderate staining of the neurohemal system on day 0. (B) Intense immunostaining by the onset of spiracular apolysis. (C) The immunostaining is almost unchanged at approximately 4 h before head-capsule slippage. (D) A pronounced decline in immunostaining is seen by the onset of head-capsule slippage. (E) Most of the immunostaining of the neurohemal system is lost by 5 h after head-capsule slippage but the cell bodies are now well stained (arrow). (F) There is a moderate increase in staining of the neurohemal system by approximately 10 h after head-capsule slippage. (G) The immunostaining continues to increase at the crochet-tanning stage. (H) At the airhead stage, immunostaining of the neurohemal system is comparable with that of the gland of the fourth-instar larva at day 0. (I) An enlargement of a portion of the neurohemal system from C, showing partly vacuous varicosities (arrows). Scale bars, 250 μm (A–H) and 10 μm (I).

mid-way through metamorphosis, MIP-immunostaining of the epiproctodeal gland cells was barely discernible (Fig. 6G), and by the adult stage, the varicosities of the neurohemal system appeared to be partly depleted (Fig. 6H).

MIP-IR neuroendocrine cells of B. mori *larvae*

Because the prothoracicostatic effect of MIP has been demonstrated only in *B. mori* (Hua et al., 1999), it was of interest to identify the MIP-IR neuroendocrine cells in this species. A single median neurosecretory cell was immunostained in each hemisphere of the larval brain (Fig. 7A; arrowhead), and this cell projects ipsilaterally (arrow) to neurohemal release sites in the corpora cardiaca (Fig. 7B). As in *M. sexta*, no neuroendocrine cells were found in the ganglia of the ventral nerve cord, and no evidence was found indicating innervation of prothoracic glands by MIP-IR axons. MIP-immunostaining demonstrated the epiproctodeal glands and their neurohemal system (Fig. 7C), and their appearance in the day 2, fourth-instar larva was much the same as that of *M. sexta*.

MIP immunoreactivity of the 704 interneurons in larvae of M. sexta *and* B. mori

In the abdominal ganglia of larvae of *M. sexta*, the antiserum to MIP labeled lateral cells located in a position very similar to that of a pair previously shown to be CCAP-immunoreactive and identified as interneurons 704 and neurosecretory cells 27 (Davis et al., 1993). Double labeling with anti-MIP and anti-CCAP demonstrated that immunoreactivities to these antisera are co-localized in the 704 interneurons (Fig. 8A,B) but not in the CCAP-IR cells 27 (Fig. 8A).

Gammie and Truman (1997) found that at the time of ecdysis, the level of CCAP immunoreactivity decreases abruptly in the 704 neurons, and so we wished to know if a

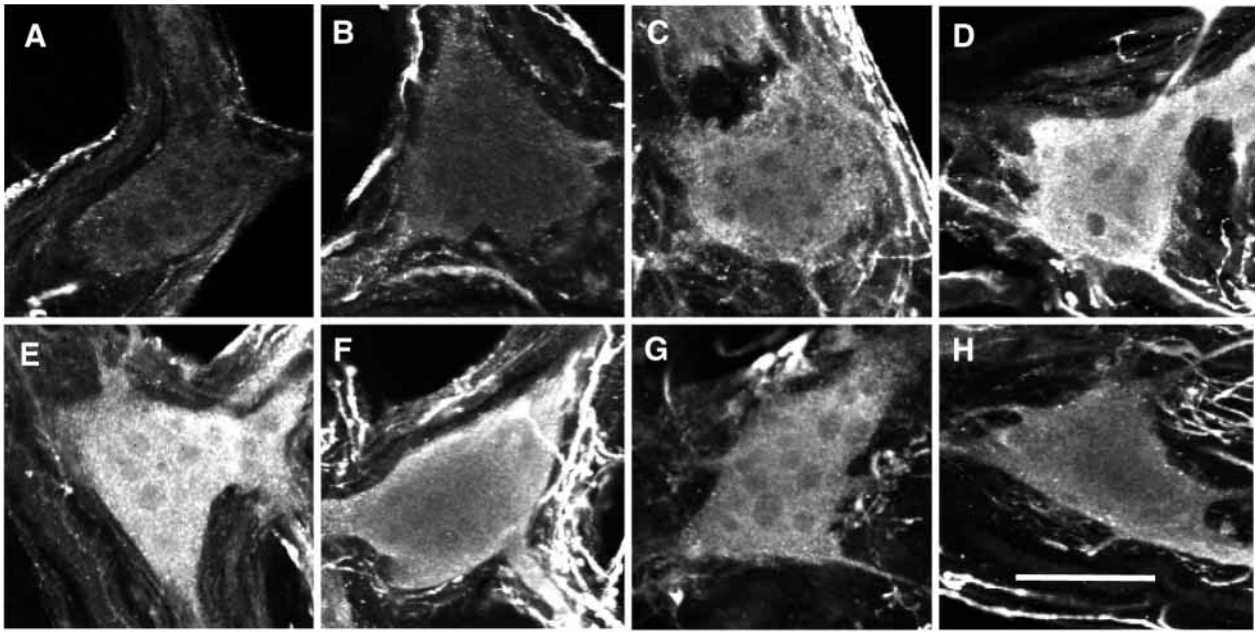

Fig. 5. Confocal images showing 5 μm optical sections through epiproctodeal gland cells. The images were made at various times in the molting cycle of fourth-instar larvae, and the changes in immunostaining indicate a period of active synthesis of the myoinhibitory peptide (MIP)-like peptide early in the molting cycle. At day 1 (A) and day 2 (B), the gland cells contain very little MIP-immunoreactive (MIP-IR) material. (C) At the onset of spiracular apolysis, distinct MIP-like immunoreactivity appears in the cytoplasm. (D) At the onset and (E) 5 h after head-capsule slippage, the MIP-like immunoreactivity is intense. (F) At 10 h after head-capsule slippage and (G) at the crochet-tanning stage, the MIP-like immunoreactivity of the cytoplasm has diminished. (H) At the airhead stage, the MIP-IR is weak and resembles that of the gland cells at the start of the fourth instar (A). Scale bar, 50 μm.

similar change occurred in the MIP immunoreactivity of the 704 neurons. Thirty abdominal ganglia of third-instar larvae at the stage of crochet tanning and thirty at the time of ecdysis were immunostained in tandem, and their confocal images were prepared using the same settings for gain and darkness. Ganglia stained several hours before ecdysis consistently showed strong MIP-immunostaining of processes in the neuropil and the somata of interneurons 704 (Fig. 8C), but at ecdysis the ganglia consistently showed a pronounced decline in immunostaining (Fig. 8D). The MIP immunoreactivity of the 704 interneurons persisted in the pharate adult (Fig. 6B,C) but was no longer present in the fully mature adult (Fig. 6D).

Unlike the abdominal ganglia of *M. sexta*, two pairs of lateral neurons were immunostained in *B. mori* (Fig. 8E), and it was not immediately apparent if either of these were comparable with the 704 neurons. Therefore, double-immunostaining was performed with the antisera to MIP and CCAP. Immunostaining of abdominal ganglia of *B. mori* for CCAP labeled pairs of lateral cells comparable with cells 27 and 704 in *M. sexta* (Fig. 8F). Double-staining indicated that CCAP-IR is co-localized with MIP-IR in the anterior pair of MIP-IR cells, and, therefore, these cells are the 704 interneurons of *B. mori* (Fig. 8G; yellow). The possible release of an MIP-like peptide from these neurons at ecdysis in *B. mori* was not studied.

Discussion

Hua et al. (1999) have shown that, *in vitro*, MIP I inhibits ecdysteroid biosynthesis by the prothoracic glands of *B. mori*. It is reasonable to expect that MIP may play a similar role in *M. sexta*, and so it is important to know how this prothoracicostatic peptide might reach receptors on the prothoracic glands in *B. mori* and *M. sexta*. Because the prothoracic glands of *B. mori* and *M. sexta* are not innervated by MIP-IR neurons, it is unlikely that the central nervous system could exert a prothoracicostatic effect directly on the prothoracic glands. Moreover, we found no evidence of release of an MIP-like peptide from neurohemal organs of the ventral nerve cord of larvae of these species. Instead, we found strong evidence that an MIP-like peptide is released as a neurohormone from the epiproctodeal glands. In *B. mori*, MIP appears to be released from both the corpora cardiaca and the epiproctodeal glands. However, the intense MIP-immunoreactivity of the epiproctodeal glands of *B. mori* suggests that these glands, as in *M. sexta*, are the principal sites of neurohemal release of MIP.

In the fourth-instar larva of *M. sexta*, the epiproctodeal glands undergo pronounced changes in secretory activity, and these changes are synchronized with the molting cycle. Immunostaining indicated that during the latter part of this cycle, an MIP-like peptide begins to accumulate in the neurohemal system of the glands (Fig. 4F,G) and that this accumulation continues into the pre-molting period (Fig. 4A,H). In fourth-instar larvae, immunostaining of the neurohemal system is most intense just before spiracular apolysis (Fig. 4B), apparently indicating a maximum

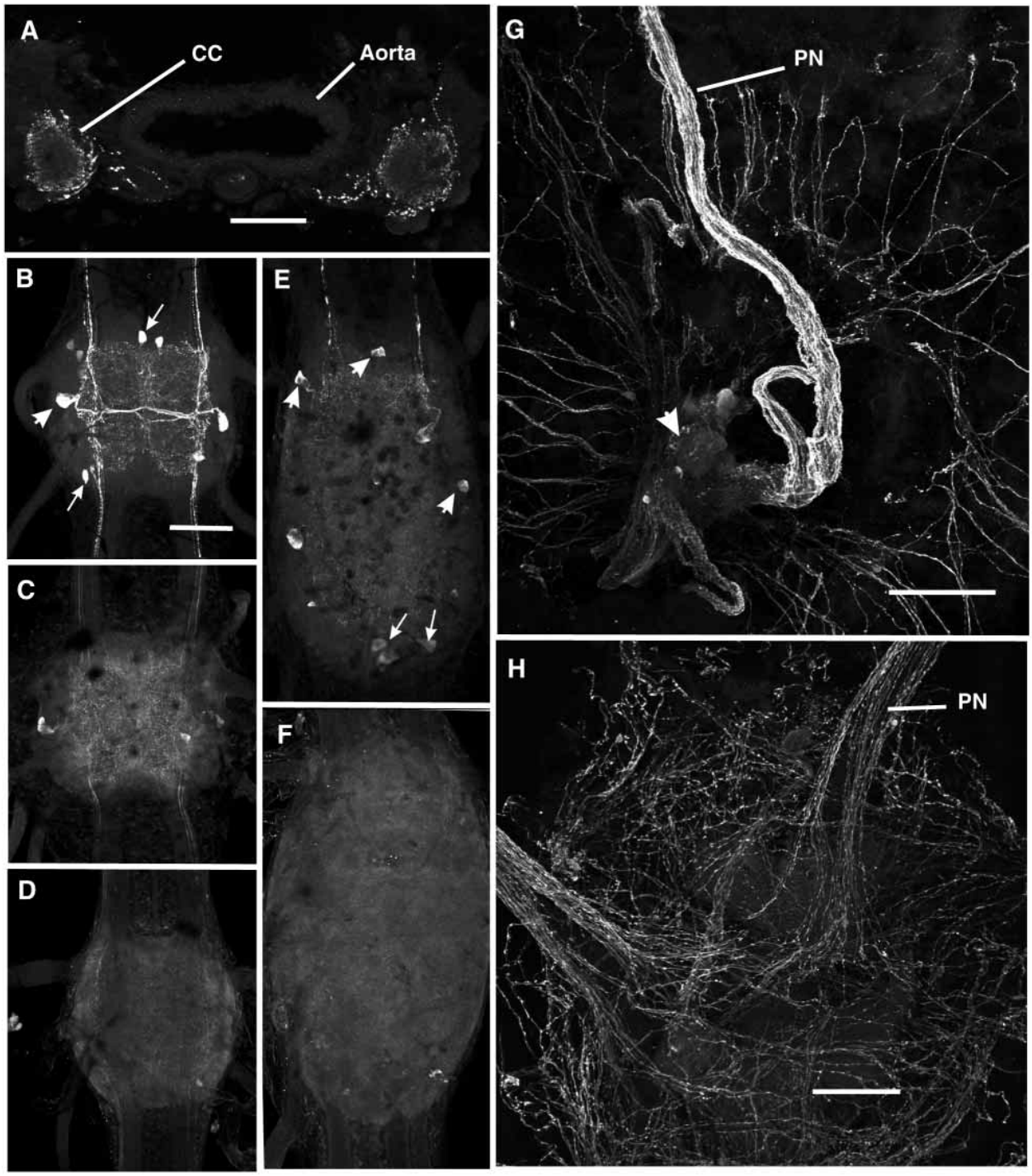

Fig. 6. Confocal images of myoinhibitory peptide-immunoreactivity (MIP-IR) in *Manduca sexta* adults. (A) Vibratome cross-section (200 μm) through the corpora cardiaca (CC) and aorta, showing immunoreactive endings near the surface of the CC. (B) Whole mount of the fifth abdominal ganglion of a pharate adult at stage-13 of development, showing strong labeling of the 704 interneurons (arrowhead), plus an anterior and posterior pair of interneurons (arrows), The latter are not labeled in the larval stages. (C) Whole mount of the fifth abdominal ganglion of a pharate adult shortly before eclosion, showing a pronounced reduction of MIP-immunostaining. (D) Whole mount of the fifth abdominal ganglion of a day-3 adult, showing an almost complete lack of staining. (E) Whole mount of the terminal abdominal ganglion of a stage-13 pharate adult, showing a reduction in MIP-immunostaining of the interneurons (arrowheads) and visceromotor neurons (arrows) (compare with Fig. 1D). (F) Whole mount of a terminal abdominal ganglion of a day-3 adult, showing an almost complete lack of MIP-immunostaining. (G) Epiproctodeal gland of a pharate adult at stage-8 of development, showing intense immunostaining of the neurohemal system on the wall of the rectum and proctodeal nerve (PN) and weak staining of the gland cells (arrowhead). (H) Whole mount of the epiproctodeal gland of a day-1 adult, showing diminished staining of the neurohemal system on the proctodeal nerves and on the wall of the rectum. At this stage, the immunostaining of the gland cells is too weak to be seen. Scale bars, 100 μm (A,H) and 200 μm (B–G).

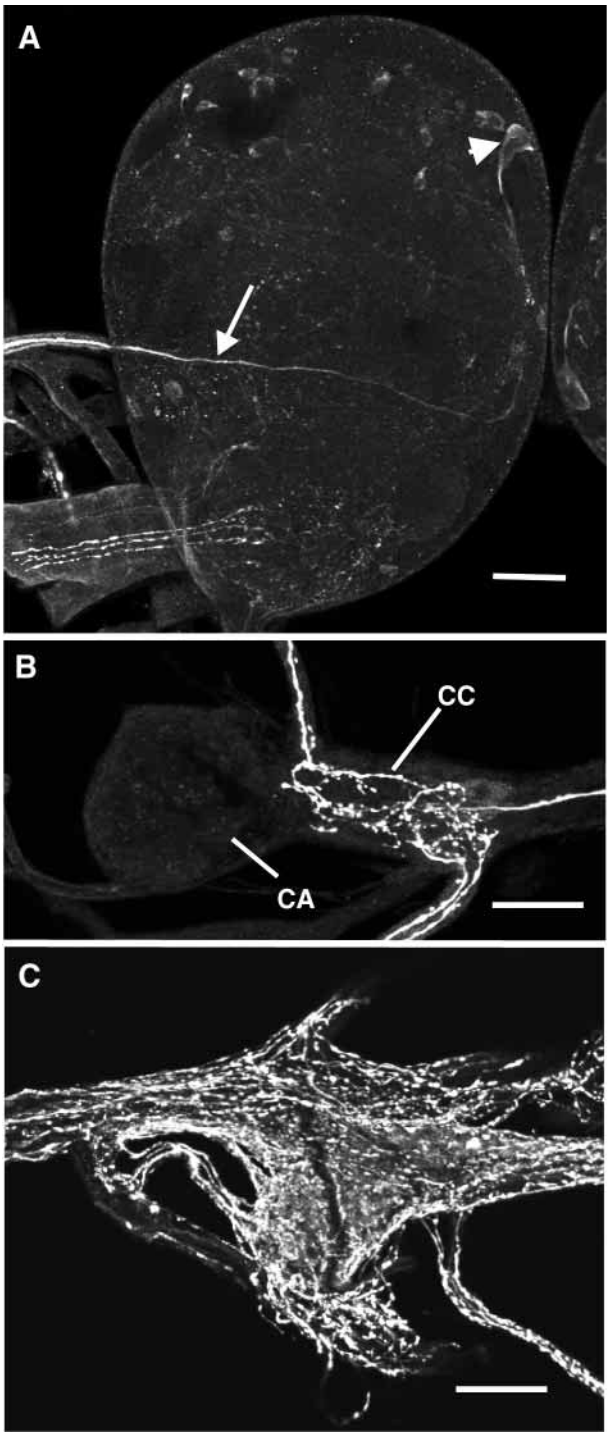

Fig. 7. Confocal images of whole mounts of myoinhibitory peptide (MIP)-like immunoreactivity in *Bombyx mori*. (A) Left hemisphere of the brain of a third-instar larva, showing an immunoreactive median neurosecretory cell (arrowhead) and its ipsilateral projection (arrow). (B) Retrocerebral complex of a third-instar larva, showing MIP-immunoreactive (MIP-IR) processes in the corpus cardiacum (CC) but not in the corpus allatum (CA). (C) Epiproctodeal gland of a fourth-instar larva showing an extensive MIP-IR neurohemal system. Scale bars, 50 μm.

accumulation of the MIP-like peptide at this time; Langelan et al. (2000) have shown that this time is near the onset of release of ecdysone from the prothoracic glands. At approximately 4 h before head-capsule slippage, the intensity of MIP-immunostaining started to decline (Fig. 4C). By the onset of head-capsule slippage, the decline in immunostaining was very pronounced and was almost complete 5 h after head-capsule slippage (Fig. 4D,E). It seems reasonable to conclude that this rapid loss of MIP-immunostaining in the neurohemal system is the result of massive release of the MIP-like peptide into the hemolymph. This period of rapid secretion (from approximately 4 h before to several hours after head-capsule slippage) corresponds exactly to the time in the molting cycle at which there is a rapid decline in the ecdysteroid titer of the fourth-instar larva (Langelan et al., 2000). Hua et al. (1999) have shown that MIP has a prothoracicostatic effect in *B. mori*, and we have demonstrated that the epiproctodeal glands are the principal source of secretion of an MIP-like peptide in *B. mori* and *M. sexta*. Therefore, we believe that this period of massive secretion by the proctodeal gland is largely responsible for the rapid decline of the ecdysteroid peak in fourth-instar larvae.

Immunostaining also appeared to demonstrate a cycle of MIP synthesis by the epiproctodeal gland cells. During the pre-molt period, there is a low level of immunostaining in the cytoplasm (Fig. 5A,B), apparently indicating that, as the neurohemal system reaches an optimum level of accumulation of the MIP-like peptide, there is a low level of synthesis (Fig. 4B). By the onset of spiracular apolysis – i.e. early in the molting cycle – the intensity of immunostaining of the gland cells increased (Fig. 5C), apparently indicating an increase in the rate of synthesis of the MIP-like peptide. The immunostaining of the cells was intense during the first few hours of head-capsule slippage (Fig. 5D,E), indicating a high rate of synthesis at this time. Then the staining indicated a gradual decline in the rate of synthesis of the MIP-like peptide (Fig. 5F–H) until it reached a level similar to that of the pre-molting phase.

The MIP-immunostaining suggested that the initiation of synthesis and release of the MIP-like peptide occurred at about the same time. The release was completed, however, in a relatively short period, while it appeared that considerable time was required for the gland cells to synthesize and transport the peptide so as to replenish the depleted neurohemal system. Our evidence from backfills indicated that the epiproctodeal glands are not innervated (Fig. 3C). Therefore, it seems very likely that the control of the glands is hormonal. Ecdysteroids are promising candidates as the source of this control, and the sudden rise in the ecdysteroid titer may initiate both synthesis and release of the MIP-like peptide by the proctodeal gland. If this hypothesis proves to be correct, then the mechanism responsible for the decline in the ecdysteroid titer in the molting cycle of the fourth-instar larva may be viewed as a delayed negative-feedback loop; ecdysteroids initiate the release of a prothoracicostatic hormone, and this hormone then inhibits release of ecdysteroids.

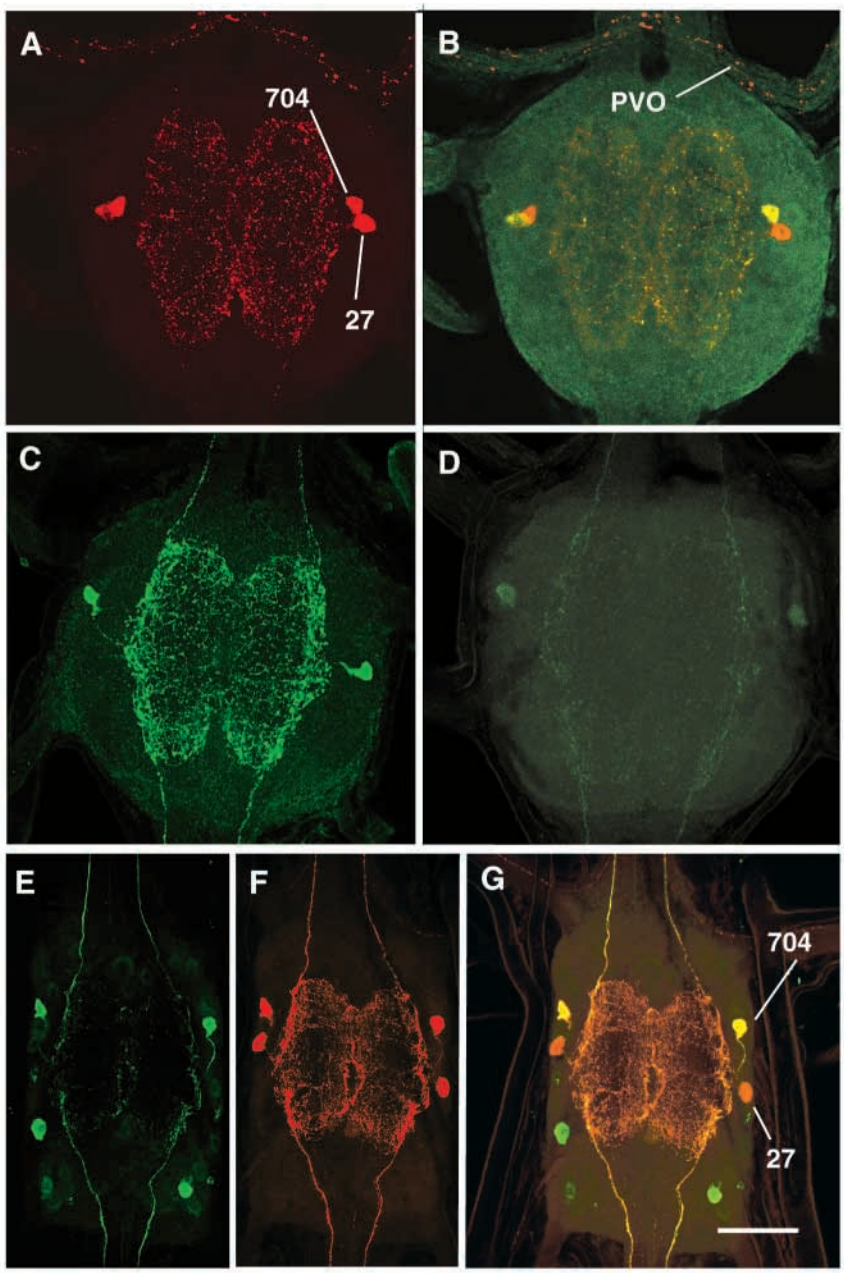

Fig. 8. Confocal images of whole mounts of the fifth abdominal ganglion of larvae of *M. sexta* and *B. mori* immunostained for crustacean cardioactive peptide (CCAP; red) and myoinhibitory peptide (MIP; green). (A) In *M. sexta*, immunostaining for CCAP demonstrated interneurons 704 and neuroendocrine cells 27, as well as processes in the neuropil and perivisceral organ (PVO). (B) In the same ganglion shown in A, double-staining for CCAP (red) and MIP (green) demonstrated that immunoreactivities to these peptides are co-localized in interneurons 704 (yellow) but not in neuroendocrine cells 27 (red). Note also that there is co-localization in much of the neuropil but not in the PVO. (C) In the abdominal ganglia of *M. sexta* larvae a few hours before ecdysis, the MIP-immunostaining of interneurons 704 and of processes in the neuropil is strong. (D) In larvae at ecdysis, the MIP-immunostaining of cells and processes is very weak, suggesting that during ecdysis the MIP-like peptide has been released. (E) In *B. mori*, MIP-immunostaining labeled two pairs of lateral cells. (F) CCAP-immunostaining of the same ganglion labeled anterior and posterior lateral somata comparable to cells 704 and 27, respectively. (G) The double-staining of this ganglion demonstrated that CCAP and MIP immunoreactivity is co-localized in interneurons 704 (yellow) but not in cells 27 (red) nor in the posterior lateral MIP-IR cells (green). Scale bars, 100 μm.

In the adult of *M. sexta*, the $1A_4$ median neuroendocrine cells were shown to be MIP-immunoreactive, and these cells are also labeled by antisera to allatostatin and diuretic hormone (Davis et al., 1997). Therefore, an MIP-like peptide may be co-released with allatostatin and diuretic hormone in the adult, but its function in the adult remains to be studied. The appearance of the epiproctodeal glands in the adult suggests that they are not functional, but it has been shown in adults of *M. sexta* that MIP inhibits the myogenic rhythm of contraction of the hindgut (Blackburn et al., 1995). Therefore, the target of MIP released from the $1A_4$ median neuroendocrine cells of the brain might be the hindgut.

In larvae of *M. sexta*, the antiserum to MIP labeled a small group of interneurons in the brain and ventral ganglia and visceromotor neurons in the terminal ganglion but did not label any neuroendocrine cells in the CNS. We have shown that the lateral pairs of 704 interneurons in the abdominal ganglia of larvae of *M. sexta*, and comparable neurons in *B. mori*, are MIP-immunoreactive, and this immunoreactivity is co-localized with that of CCAP. Ewer et al. (1998) have demonstrated cell death of the 704 interneurons in fully mature *M. sexta* adults, and, as expected, we have found that in adults, these cells are not labeled by MIP-immunostaining.

In *M. sexta*, the level of MIP-IR in the 704 interneurons decreases at the time of larval ecdysis, and Gammie and Truman (1997) reported a similar decrease in CCAP-IR. Moreover, these authors showed that application of CCAP to de-sheathed abdominal ganglia results in generation of

rhythmic bursts of impulses associated with the ecdysis motor program, apparently indicating that release of CCAP from the 704 interneurons activates this motor program. Our results strongly suggest that MIP and CCAP are co-released at the time of ecdysis and that MIP may also be involved in the initiation of the ecdysis motor program.

References

Blackburn, M. B., Jaffe, H., Kochansky, J. and Raina, A. K. (2001). Identification of four additional myoinhibitory peptides (MIPs) from the ventral nerve cord of *Manduca sexta*. *Arch. Insect Biochem. Physiol.* **48**, 121-128.

Blackburn, M. B., Wagner, R. M., Kochansky, J. P., Harrison, D. J., Thomas-Laemont, P. and Raina, A. (1995). Identification of two myoinhibitory peptides, with sequence similarities to the galanins, isolated from the ventral nerve cord of *Manduca sexta*. *Regul. Pept.* **57**, 213-219.

Bollenbacher, W. E. and Granger, N. A. (1985). Endocrinology of the prothoracicotropic hormone. In *Comprehensive Insect Physiology, Biochemistry and Pharmacology*, vol. 7 (ed. G. A. Kurkut and L. I. Gilbert), pp. 105-151. New York: Pergamon Press.

Bollenbacher, W. E., Smith, S. L., Goodman, W. and Gilbert, L. I. (1981). Ecdysteroid titer during larval–pupal–adult development of the tobacco hornworm, *Manduca sexta*. *Gen. Comp. Endocrinol*. **44**, 302-306.

Consoulas, C., Johnson, R. M., Pflüger, H. J. and Levine, R. B. (1999). Peripheral distribution of presynaptic sites of abdominal motor and modulatory neurons in *Manduca sexta* larvae. *J. Comp. Neurol*. **410**, 4-19.

Curtis, A. T., Hori, M., Green, J. M., Wolfgang, W. J., Hiruma, K. and Riddiford, L. M. (1984). Ecdysteroid regulation of the onset of cuticular melanization in allectomized and *black* mutant *Manduca sexta* larvae. *J. Insect Physiol.* **30**, 597-606.

Davis, N. T., Homberg, U., Dircksen, H., Levine, R. B. and Hildebrand, J. G. (1993). Crustacean cardioactive peptide-immunoreactive neurons in the hawkmoth *Manduca sexta* and changes in their immunoreactivity during postembryonic development. *J. Comp. Neurol*. **338**, 612-627.

Davis, N. T., Veenstra, J. A., Feyereisen, R. and Hildebrand, J. G. (1997). Allatostatin- like-immunoreactive neurons in the tobacco hornworm, *Manduca sexta*, and isolation and identification of a new neuropeptide related to cockroach allatostatins. *J. Comp. Neurol*. **385**, 265-284.

Dedos, S. G., Nagata, S., Ito, J. and Takamiya, M. (2001). Action kinetics of a prothoracicostatic peptide from *Bombyx mori* and its possible signaling pathway. *Gen. Comp. Endocrinol*. **122**, 98-108.

Ewer, J., Wang, C.-M., Klukas, K. A., Mesce, K. A., Truman, J. W. and Fahrbach, S. E. (1998). Programmed cell death of identified peptidergic neurons involved in ecdysis behavior in the moth, *Manduca sexta*. *J. Neurobiol.* **37**, 265-280.

Fain, M. J. and Riddiford, L. M. (1975). Juvenile hormone titers in the hemolymph during late larval development of the tobacco hornworm, *Manduca sexta*. *Biol. Bull.* **149**, 506-521.

Gäde, G., Hoffmann, K. H. and Spring, J. H. (1997). Hormonal regulation in insects: facts, gaps, and future directions. *Physiol. Rev.* **77**, 963-1032.

Gammie, S. C. and Truman, J. W. (1997). Neuropeptide hierarchies and the activation of sequential motor behaviors in the hawkmoth, *Manduca sexta*. *J. Neurosci.* **17**, 4389-4397.

Hewes, R. S. and Truman, J. W. (1994). Steroid regulation of excitability of identified neurosecretory cells. *J. Neurosci.* **14**, 1812-1819.

Homberg, U., Davis, N. T. and Hildebrand, J. G. (1991). Peptide-immunohistochemistry of neurosecretory cells in the brain and retrocerebral complex of the sphinx moth, *Manduca sexta*. *J. Comp. Neurol.* **303**, 35-52.

Hua, Y.-J., Tanaka, Y. and Kataoka, H. (2000). Molecular cloning of a prothoracicostatic peptide (PTSP) in the larval brain of the silkworm, *Bombyx mori*. *XXI Internat. Cong. Entomol.* **2**, 884 (Abstr.).

Hua, Y.-J., Tanaka, Y., Nakamura, K., Sakakibara, M., Nagata, S. and Kataoka, H. (1999). Identification of a prothoracicostatic peptide in the larval brain of the silkworm, *Bombyx mori*. *J. Biol. Chem.* **247**, 31169-31173.

Kiernan, J A. (1990). *Histological and Histochemical Methods: Theory and Practice*. 2nd edition. Oxford: Pergamon Press.

Kingan, T. G. and Adams, M. E. (2000). Ecdysteroids regulate secretory competence in inka cells. *J. Exp. Biol.* **203**, 3011-3018.

Langelan, R. E., Fisher, J. E., Hiruma, K., Palli, S. R. and Riddiford, L. M. (2000). Patterns of MHR3 expression in the epidermis during a larval molt of the tobacco hornworm *Manduca sexta*. *Dev. Biol.* **227**, 481-494.

Lorenz, M. W., Kellner, R. and Hoffman, K. H. (1995). A family of neuropeptides that inhibit juvenile hormone biosynthesis in the cricket, *Gryllus bimaculatus*. *J. Biol. Chem.* **270**, 21103-21108.

Lorenz, M. W., Kellner, R., Hoffman, K. H. and Gäde, G. (2000). Identification of multiple peptides homologous to cockroach and cricket allatostatins in the stick insect *Carausius morosus*. *Insect Biochem. Mol. Biol.* **30**, 711-718.

Nichols, R., McCormick, J. and Caserta, L. (1995b). Cellular expression of the *Drosophila* neuropeptide DPKQDFMRFamide: evidence for differential processing of the FMRFamide polypeptide precursor. *J. Mol. Neurosci.* **6**, 1-10.

Nichols, R., McCormick, J., Lim, I. and Starkman, J. (1995a). Spatial and temporal analysis of the *Drosophila* FMRFamide neuropeptide gene product SDNFMRFamide: evidence for a restricted cellular expression pattern. *Neuropeptides* **29**, 205-213.

Nijhout, H. F. (1994). *Insect Hormones.* Princeton: Princeton University Press.

Pichon, Y., Sattelle, D. B. and Lane, N. J. (1972). Conduction processes in the nerve cord of the moth *Manduca sexta* in relation to its ultrastructure and haemolymph ionic composition. *J. Exp. Biol.* **56**, 717-734.

Predel, R., Rapus, J. and Eckert, M. (2001). Myoinhibitory neuropeptides in the American cockroach. *Peptides* **22**, 199-208.

Reinecke, J. P., Gerst, J., O'Gara, B. and Adams, T. S. (1978). Innervation of hindgut muscle of larval *Manduca sexta* (L.) (Lepidoptera: Sphingidae) by a peripheral neurosecretory neuron. *Int. J. Insect Morphol. Embryol.* **7**, 435-453.

Schoofs, L., Holman, G. M., Hayes, T. K., Nachman, R. J. and De Loof, A. (1991). Isolation, identification and synthesis of locustamyoinhibiting peptide (Lom-MIP), a novel biologically active peptide from *Locusta migratoria*. *Regul. Pept.* **36**, 111-119.

Schwartz, L. M. and Truman, J. W. (1983). Hormonal control of rates of metamorphic development in the tobacco hornworm, *Manduca sexta*. *Dev. Biol.* **99**, 103-114.

Sláma, K. (1980). Homeostatic function of ecdysteroids in ecdysis and oviposition. *Acta Entomol. Bohem.* **77**, 145-168.

Triseleva, T. A. and Golubeva, E. G. (1998). Immunohistochemical localization of myoinhibitory Mas-MIP-I-like peptides in *Heliothis virescens* (F.) (Lepidoptera, Noctuidae). *Biology Bull.* **25**, 588-591. [Translated from Russian in **Triseleva, T. A. and Golubeva, E. G.** (1998). *Izvestiya Akademii Nauk, Seriya Biologicheskaya*, **6**, 712-716.]

Truman, J. W. (1972). Physiology of insect rhythms. I. Circadian organization of the endocrine events underlying the moulting cycle of larval tobacco hornworms. *J. Exp. Biol.* **57**, 805-820.

Truman, J. W. and Morton, D. B. (1990). The eclosion hormone system: an example of coordination of endocrine activity during the molting cycle of insects. *Prog. Clin. Biol. Res.* **342**, 300-308.

Truman, J. W., Roundtree, D. B., Reiss, S. E. and Schwartz, L. M. (1983). Ecdysteroids regulate the release and action of eclosion hormone in the tobacco hornworm, *Manduca sexta* (L.). *J. Insect Physiol.* **29**, 895-900.

Williamson, M., Lenz, C., Winther, M. E., Nässel, D. R. and Grimmelikhuijzen, C. J. P. (2001). Molecular cloning, genomic organization, and expression of a B-type (cricket-type) allatostatin preprohormone from *Drosophila melanogaster*. *Biochem. Biophys. Res. Commun.* **281**, 544-550.

Žitňan, D., Ross, L. S., Žitňanova, I., Hermesman, J. L., Gill, S. and Adams, M. E. (1999). Steroid induction of a peptide hormone gene leads to orchestration of a defined behavioral sequence. *Neuron* **23**, 523-535.